Figures and tables

ec0005
Supplementary Fig. 1
Supplementary Fig. 2
Supplementary Fig. 3
Supplementary Fig. 4

Chemical Geology
Volume 373, 12 May 2014, Pages 1–9

EXHIBIT PP

Isotopic evidence for reduction of anthropogenic hexavalent chromium in Los Alamos National Laboratory groundwater

Jeffrey M. Heikoop[a], , Thomas M. Johnson[b], Kay H. Birdsell[a], Patrick Longmire[a, 1], Donald D. Hickmott[a], Elaine P. Jacobs[a], David E. Broxton[a], Danny Katzman[c], Velimir V. Vesselinov[a], Mei Ding[a], David T. Vaniman[a], Steven L. Reneau[a], Tim J. Goering[c], Justin Glessner[b, 2], Anirban Basu[b, 3]

doi:10.1016/j.chemgeo.2014.02.022

Highlights

- Study using Cr isotopes in groundwater to characterize contaminant attenuation
- Cr isotopes indicate chromate reduction between surface and regional groundwater.
- Chromate reduction is most strongly associated with basalts.

Abstract

Reduction of toxic Cr(VI) to less toxic Cr(III) is an important process for attenuating Cr(VI) transport in groundwater. This process results in immobilization of chromium as Cr(III) and effectively decreases the overall mobility of the chromium inventory. During both abiotic and biotic reduction of Cr(VI) to Cr(III), a kinetic isotope effect occurs in which the lighter isotope, ^{52}Cr, reacts preferentially, leaving the remaining dissolved Cr(VI) enriched in the heavier isotope, ^{53}Cr. Cr isotopes have proven to be a useful tool for estimating the magnitude of Cr(VI) reduction and for determining where in a hydrologic system reduction is occurring. In this paper, we discuss patterns of reduction in perched-intermediate and regional aquifer systems contaminated with Cr(VI) related to historical use of potassium dichromate as an anticorrosion agent in cooling towers at a power plant at the Los Alamos National Laboratory in northern New Mexico. We utilize Cr isotopes to assess the relative effects of mixing and reduction on measured $\delta^{53}Cr$ in groundwater, with an emphasis on where in the system reduction occurs. Chromium isotope measurements provide strong evidence for reduction of Cr(VI) in vadose zone basalts.

Abbreviations

LANL, Los Alamos National Laboratory; RLWTF, Radioactive Liquid Waste Treatment Facility; TA, Technical Area

Keywords

Chromium; Contamination; Chromium isotopes; Reduction; Groundwater

1. Introduction

Reduction of toxic Cr(VI) to less toxic Cr(III) is an important process for attenuating Cr(VI) transport in groundwater (Eary and Rai, 1989, Palmer and Wittbrodt, 1991, Palmer and Puls, 1994 and Davis and Olsen, 1995). This process results in immobilization of

chromium as Cr(III) and effectively decreases the overall mobility of the chromium inventory. Cr isotopes have proven to be a useful tool for estimating the magnitude of Cr(VI) reduction and for determining where in a hydrologic system reduction is occurring (Blowes, 2002, Ellis et al., 2002, Izbicki et al., 2008, Izbicki et al., 2012, Berna et al., 2010, Gao et al., 2010, Raddatz et al., 2011, Wanner et al., 2012a and Wanner et al., 2012b).

The use of Cr isotopes to estimate the magnitude of Cr(VI) reduction along a flow path relies on the fact that during both abiotic and biotic reduction of Cr(VI) to Cr(III), a kinetic isotope effect occurs in which the lighter isotope, ^{52}Cr, reacts preferentially, leaving the remaining dissolved Cr(VI) enriched in the heavier isotope, ^{53}Cr (e.g. Ellis et al., 2002, Johnson and Bullen, 2004, Izbicki et al., 2008, Berna et al., 2010 and Jamieson-Hanes et al., 2012b). The most common model used to determine the extent of reduction based on the $\delta^{53}Cr$ of Cr(VI) is the Rayleigh model (Ellis et al., 2002, Berna et al., 2010, Zink et al., 2010, Dossing et al., 2011 and Raddatz et al., 2011) that can be closely approximated as

$$\delta = \delta_0 - \varepsilon \ln(f) \quad (1)$$

(see Supplementary Information for an explanation of delta notation)where δ is the measured $\delta^{53}Cr$ value, δ_0 is the initial $\delta^{53}Cr$ value prior to any reduction, f is the fraction of the original Cr(VI) remaining, and ε expresses the magnitude of isotopic fractionation (Raddatz et al., 2011). ε can be expressed in per mil form and approximated as

$$\varepsilon = \delta^{53}Cr_{reactant} - \delta^{53}Cr_{product}. \quad (2)$$

Application of the Rayleigh model to determine the magnitude of Cr(VI) reduction can be considered semi-quantitative as a range of experimental ε values has been determined in laboratory experiments using inorganic and organic reductants and biotic and abiotic reduction mechanisms. The range of Cr isotopic fractionation determined in batch and column experiments is ε = 0.4 to 5‰ (Ellis et al., 2002, Sikora et al., 2008, Berna et al., 2010, Zink et al., 2010, Dossing et al., 2011, Basu and Johnson, 2012, Han et al., 2012, Jamieson-Hanes et al., 2012b and Kitchen et al., 2012). Fractionation tends to be smaller in cases of rapid Cr(VI) reduction (Kitchen et al., 2012), anaerobic microbial reduction (Sikora et al., 2008), reduction during porous flow (in column studies) (Jamieson-Hanes et al., 2012a and Jamieson-Hanes et al., 2012b), and when there is addition of fresh reductant at constant mass flux (Dossing et al., 2011). Additionally, ε values determined based on field experiments tend to fall on the lower end of the observed range of laboratory-derived values (Berna et al., 2010, Izbicki et al., 2012 and Wanner et al., 2012a). If actual aquifer fractionation is lower than assumed by applying Eq. (1), the degree of reduction will be underestimated. Since the particular reduction mechanism and associated ε value are typically unknown for a given groundwater setting, there is considerable uncertainty in estimation of the magnitude of reduction (Jamieson-Hanes et al., 2012a and Jamieson-Hanes et al., 2012b). Cr isotope measurements, however, still provide important bounds on the degree of natural reduction in groundwater systems, including where in the system reduction is most prevalent.

Chromium isotopic fractionation does not appear to vary with Cr(VI) concentration, at least in the case of microbial reduction (Sikora et al., 2008). In addition, there does not appear to be isotopic exchange between Cr(III) and Cr(VI) on short timescales of days to weeks (Zink et al., 2010). Also, Cr isotopes are not fractionated significantly by sorption processes (Ellis et al., 2004).

In some settings, mixing of natural and anthropogenic Cr(VI) must be considered (e.g. Raddatz et al., 2011). Recent work suggests that water–rock interactions during weathering of mafic rocks result in the production of natural Cr(VI) with elevated $\delta^{53}Cr$ (Izbicki et al., 2008). Alternatively, elevation of $\delta^{53}Cr$ in naturally-sourced dissolved Cr(VI) can occur after Cr(VI) "is delivered to the water, via partial reduction by Fe(II)-bearing solids or bacteria" (Raddatz et al., 2011). Chromite ores, from which industrial Cr is derived, have an average $\delta^{53}Cr$ of −0.082 ± 0.058‰ (2 σ) (Schoenberg et al., 2008). Because of the high temperature and efficiency of Cr extraction from ore, industrial Cr should have very similar $\delta^{53}Cr$ values to chromite ore (Ellis et al., 2002 and Schoenberg

et al., 2008). The highest value measured in industrial reagent Cr was 0.37‰ (Ellis et al., 2002). Uncertainty in the $\delta^{53}Cr$ of the industrial source adds further uncertainty in calculating the degree of Cr(VI) reduction occurring along a flow path.

At present, only a small number of case studies have been published to describe application of Cr isotopes in practical field studies. Herein, we discuss patterns of reduction in perched-intermediate and regional aquifer systems contaminated with Cr (VI) related to historical use of potassium dichromate as an anticorrosion agent in cooling towers at a power plant at the Los Alamos National Laboratory (LANL) in northern New Mexico. Potassium dichromate was a common industrial corrosion inhibitor when it was used at LANL. The subsurface stratigraphy in this setting includes basalts with Fe(II)-bearing minerals and other rock types where natural attenuation via reduction of Cr(VI) may occur. Cr(VI) reduction in basalts at the Idaho National Laboratory has been suggested based on evidence from Cr isotopes (Raddatz et al., 2011). Natural Cr(VI) occurs in groundwater at the LANL site (Dale et al., 2013), so the effect of mixing between natural and anthropogenic sources must be considered. We apply the approach utilized by Raddatz et al. (2011) to assess the relative effects of mixing and reduction on measured $\delta^{53}Cr$ in LANL groundwater, with an emphasis on where in the system reduction occurs.

1.1. Discharge of hexavalent chromium and other contaminants

Fig. 1 shows the location of liquid outfalls relevant to this investigation. Liquid effluents have been discharged to Sandia Canyon since the early 1950s at Outfall 001. The highest volume releases include treated sanitary wastewater, steam plant effluent, and cooling tower blowdown from the LANL Technical Area 3 (TA-03) power plant. Potassium dichromate was used from 1956 to 1972, and resulted in an estimated total release of 31,000 to 72,000 kg of Cr(VI) into upper Sandia Canyon. Outfall discharge during this period is estimated at 0.4 to 1.1 million liters per day. Recent outfall discharge to upper Sandia Canyon is approximately 0.8 to 1.5 million liters per day, providing sufficient water to mobilize contaminants within the watershed (LANL, 2009 and LANL, 2012).

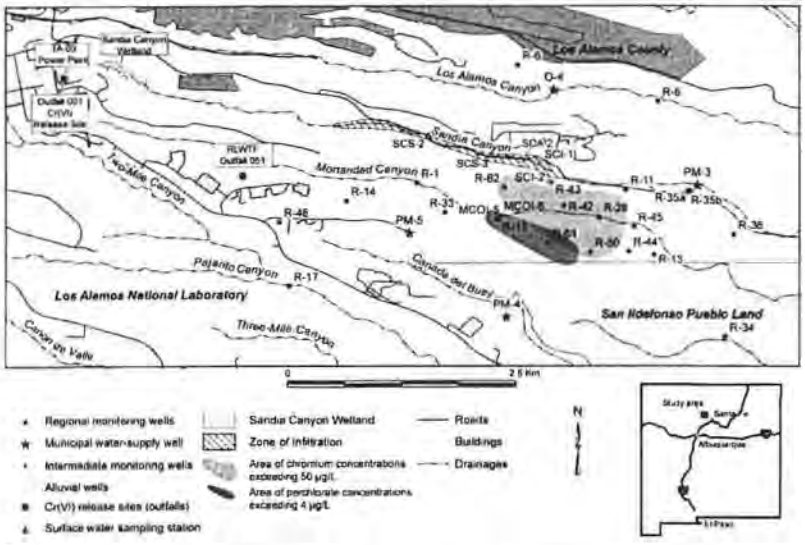

Fig. 1.
Location map showing outfalls, the Sandia Canyon wetland, the primary Cr(VI) infiltration zone, locations of monitoring wells, the area of Cr(VI) concentration exceeding 50 µg/L in the regional aquifer, and the area of perchlorate concentration exceeding 4 µg/L in the regional aquifer. Wells R-10 and R-10a are off the map to the east, outside the area of influence of the Cr plume.

Figure options

Contaminant discharges to Mortandad Canyon, located to the south of Sandia Canyon (Fig. 1), are also relevant to this investigation due to the potential for mixing with waters originating in Sandia Canyon. Water treatment at LANL's Radioactive Liquid Waste Treatment Facility (RLWTF) began in July 1963. The RLWTF discharged treated

wastewater containing perchlorate, nitrate and tritium, but not Cr(VI), to Mortandad Canyon through Outfall 051 via a tributary called Effluent Canyon. However, a smaller chromium source (based on the occurrence of Cr(III) in sediments) of unknown provenance also occurs in Effluent Canyon upgradient from Outfall 051. Outfall 051 has historically released much lower volumes of effluent than Outfall 001 with peak discharges of 0.2 million liters per day occurring in 1968. Discharges from Outfall 051 decreased significantly after the mid-1980s and effectively ended in late 2010 (LANL, 2009 and LANL, 2012).

1.2. Conceptual model for chromium transport

This section is summarized from recent regulatory reports submitted to the New Mexico Environment Department (LANL, 2009 and LANL, 2012; reports are publicly available (see http://www.lanl.gov/community-environment/environmental-stewardship/public-reading-room.php); see also Birdsell et al. (2005) and Vesselinov et al. (2013)). LANL groundwater data may be accessed online at www.intellusnm.com.

A significant portion of the Cr(VI) released from Outfall 001 to Sandia Canyon was immobilized as Cr(III) in a wetland present in the upper part of Sandia Canyon (Fig. 1). The estimated total inventory of contaminant chromium in sediment deposits in Sandia Canyon is 18,000 kg, with measured concentrations ranging from 5.6 mg/kg to 3740 mg/kg (LANL, 2007). Approximately eighty-five percent of this total is concentrated in sediments within the Sandia Canyon wetland. Chromium in wetland sediments is nearly 100% Cr(III) based on paired analyses of total Cr and Cr(VI) (LANL, 2007).

A water balance study in Sandia Canyon showed that most surface water passes through the wetland area, with less than 2% of the water lost to evapotranspiration and infiltration (LANL, 2009). After exiting the wetland, surface water flows without loss approximately 0.85 km down a narrow slot canyon underlain by relatively impermeable welded tuff with little or no alluvial sediments. About 20% of the surface water infiltrates the canyon floor between 0.85 and 3.6 km east of the wetland. Approximately 60% infiltrates 3.6 to 4.5 km east of the wetland where the canyon gradually widens and alluvial deposits become about 20 m thick. The infiltrated surface water forms a perched alluvial groundwater system that extends down canyon approximately 2.2 km (Fig. 1, Supplementary Fig. 1). The alluvial groundwater drains into the suballuvial bedrock tuffs that are poorly welded and more porous in this part of the canyon. Flow into the suballuvial bedrock is spatially and temporally heterogeneous with percolation rates potentially as high as a few meters per year, resulting in travel times to the regional aquifer from 5 to 50 years with best estimates ranging between 20 to 30 years. Deeper percolation of alluvial groundwater as unsaturated flow provides a driving force for subsurface transport of mobile constituents, including Cr(VI).

From the alluvial zone, water percolates down through the vadose zone, consisting of Bandelier Tuff Formation volcanic rocks and Puye Formation sediments, where perching horizons on top of and within Cerros del Rio basalts cause some water to move laterally (Supplementary Fig. 1; For a detailed description of site geology see Broxton and Vaniman, 2005). The perching horizons in these basalts dip towards the south and southwest causing the perched-intermediate groundwater to flow toward Mortandad Canyon. Percolation through the basalts is expected to be dominated by unsaturated flow through fractured matrix and interflow breccias. Leakage from the perched zones occurs as water flows laterally, and contaminants migrate downward toward the regional aquifer. Percolation in the lower vadose zone is probably dominated by gravity-driven flow through highly porous sediments of the lower Puye Formation and underlying older Miocene-age pumiceous deposits.

Chromium released into Sandia Canyon in the mid-1950s through early 1970s has migrated along these pathways and is observed in the regional aquifer beneath Sandia Canyon and Mortandad Canyon at concentrations that exceed the New Mexico groundwater standard of 50 μg/L (Fig. 2). The zone of contamination is confined to the upper portions of the regional aquifer. Contaminant transport in the regional aquifer is believed to predominantly follow shallow water table gradients with relatively poor hydraulic communication with deeper aquifer zones, though this does not preclude some

migration of Cr(VI) between zones (Vesselinov et al., 2013).

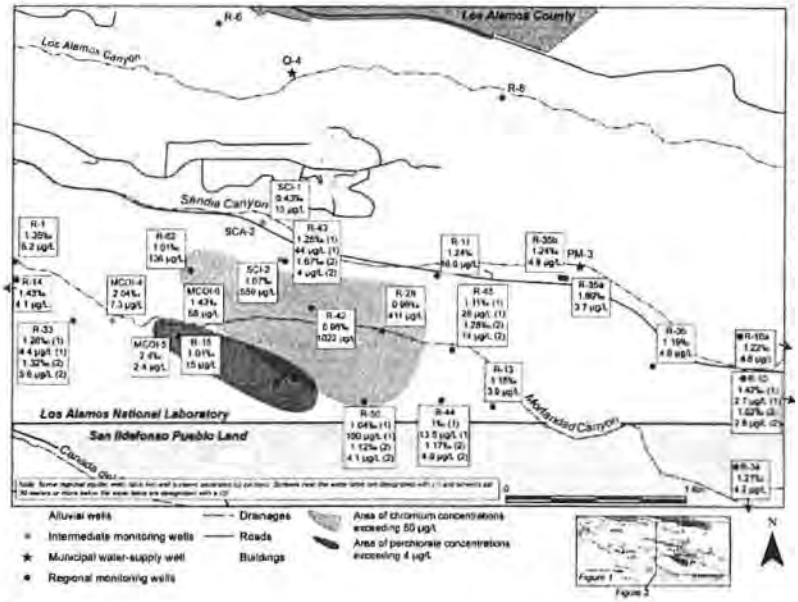

Fig. 2.

Most recent $\delta^{53}Cr$ and Cr(VI) concentrations for perched-intermediate and regional aquifer wells in Sandia Canyon and Mortandad Canyon (sample dates from 2008–2012). Where two values are given for each parameter, those followed by (1) are from the upper screen and those followed by (2) from the lower screen of the particular well (see Supplementary Table 1 for screen depths). Text boxes shaded in yellow represent wells outside the Cr plume that have only natural background chromate present. The pink-shaded plume represents the area of the regional groundwater system where Cr(VI) concentrations are above the New Mexico groundwater standard of 50 µg/L. The gray-shaded plume represents the area of the regional groundwater system where perchlorate concentrations are above a New Mexico screening level of 4 µg/L.

Figure options

Data from groundwater monitoring wells reveals the presence of two geochemically distinct groundwater plumes, one derived from a Sandia Canyon source (with elevated chromium as a key indicator) and one derived from a Mortandad Canyon source (with elevated perchlorate as a key indicator) (Fig. 1). Mixing of these plumes occurs in perched-intermediate (110–210 meter depth) and regional groundwater (260–380 meter depth) beneath and to the south of Mortandad Canyon. For example, perched-intermediate wells MCOI-4, MCOI-5 and MCOI-6 located in Mortandad Canyon (Fig. 2) all contain perchlorate, nitrate, and tritium, contaminants released by the RLWTF at Outfall 051. However, well MCOI-6 contains elevated chromium in addition to the RLWTF contaminants, indicating that it is recharged by water originating from both Sandia and Mortandad Canyons. Recent declines in water levels at well MCOI-6 correspond with declining perchlorate, nitrate, and tritium concentrations. However, Cr concentrations have simultaneously increased, likely reflecting improved water quality and lower effluent volumes from Outfall 051 (Mortandad Canyon) resulting in a subsequent increase in the fraction of Sandia Canyon derived water. The observed trends support the conceptual model of perched-intermediate groundwater flow to the south and southwest from Sandia Canyon towards Mortandad Canyon.

Geochemical indicators also link perched-intermediate groundwater at well SCI-2 in Sandia Canyon to regional groundwater at wells R-28, R-42 and R-50 in Mortandad Canyon, which are in the centroid of the Cr plume as defined by the 50 µg/L-contour (Fig. 2). Concentrations indicate that Cr enters the regional aquifer near wells R-42 and R-28 (Vesselinov et al., 2013). A simplified hypothetical subsurface flow path for Cr(VI) contamination, therefore, includes vertical flow from perched alluvial groundwater in Sandia Canyon to perched-intermediate groundwater on top of (e.g. at well SCI-1) and within (e.g. at well SCI-2) the Cerros del Rio basalts, and south to southwest lateral flow of perched-intermediate groundwater before it drops to the regional aquifer near wells R-42 and R-28. In reality, there are likely multiple flow paths and arrival points to the

regional aquifer (Vesselinov et al., 2013) and perhaps mixing with secondary, less significant, Cr(VI) from a Mortandad Canyon source.

2. Methods

Groundwater samples were collected at perched-intermediate and regional monitoring wells (Fig. 2) in 1-L high-density polypropylene bottles. Before November 2008, the non-acidified samples were filtered through 0.45-micrometer membranes. During the course of this investigation, it was recognized that, for some samples, colloidal Cr(III) passed through 0.45 and 0.22-micrometer membranes. Even though colloidal Cr(III) appears to have no measurable effect on $\delta^{53}Cr$ of Cr(VI) (LANL, 2009), samples collected since November 2008 have been filtered through 0.02-micrometer membranes.

All samples were analyzed for Cr isotope ratios and concentrations on a Nu Plasma HR MC-ICP-MS (multicollector inductively coupled plasma mass spectrometer) at the University of Illinois-Urbana Champaign using a $^{54}Cr/^{50}Cr$ double isotope spike technique (Ellis et al., 2002, Johnson and Bullen, 2004 and Schoenberg et al., 2008). For a detailed description of sample preparation and analytical techniques see Raddatz et al. (2011). The absolute difference between duplicate pairs of field samples was always below 0.2‰, except for one sample from well R-35a where the difference in duplicates was 0.23‰. Two times the root-mean-square difference for 16 pairs of duplicate samples was ± 0.13‰ (95% confidence). Cr(VI) concentrations were determined by isotope dilution against the double spike solution. The ^{54}Cr concentration of the double spike is calibrated, and the volumes of the sample and the added spike are measured precisely. The measured $^{54}Cr/^{52}Cr$ ratio, corrected for mass bias, provides a precise indication of sample concentration relative to spike concentration, using standard isotope dilution calculations.

No samples of the potassium dichromate used in the TA-03 cooling tower were available for analysis. Potassium dichromate solutions used by Jamieson-Hanes et al. (2012b) in batch and column experiments were close to 0‰. Here we assume a value of 0‰ for δ_0 of contaminant Cr(VI), consistent with measurements of industrial chromate solutions (Ellis et al., 2002 and Schoenberg et al., 2008).

3. Results and discussion

Values for $\delta^{53}Cr$ and Cr(VI) concentrations of groundwater samples are presented in Supplementary Table 1 of the Supplementary information. Well locations are provided in Supplementary Table 2. Spatial variability in results is shown in Fig. 2. Because the wells sampled were installed over many years, data from the most recent sampling events are shown in Fig. 2 (as opposed to averages). For the majority of wells, particularly those completed in the regional aquifer, $\delta^{53}Cr$ is relatively consistent over time (Supplementary Table 1). Notable exceptions include the shallow screen at regional aquifer well R-43 and both screens at regional aquifer well R-45, which are discussed in more detail in Section 3.4. Intermediate well MCOI-6 also shows isotopic variation through time, although insufficient isotopic data exist to evaluate trends. All three of these wells are located at the margin of the plume where dynamic geochemical behavior is expected.

3.1. Potential locations for reduction of Cr(VI)

From a remediation standpoint, it is desirable to know where in the system natural attenuation of chromate is occurring. The primary locations where Cr(VI) may be reduced to Cr(III) include 1) the cooling towers (which could affect the $\delta^{53}Cr$ signal of Cr(VI) input into the natural environment), 2) the Sandia Canyon wetland, 3) the vadose zone, and 4) the regional aquifer.

The degree of Cr isotopic fractionation associated with the use of chromate in cooling towers as a corrosion inhibitor is expected to be limited due to the constant replenishment of Cr(VI) necessitated by constant losses of cooling water. Thus the $\delta^{53}Cr$ of Cr(VI) associated with cooling water outflow is expected to be near zero.

Cr(VI) reduction is prevalent in the Sandia Canyon wetland where the current inventory of Cr(III) is estimated at 15,000 kg (LANL, 2007). In our preferred conceptual model we

assume that all Cr(VI) interacting with wetland sediments is reduced to Cr(III), leaving no or only minor residual Cr(VI) with a higher $\delta^{53}Cr$ signature. Contaminant Cr(VI) detected further down the flow path is likely derived from fast-moving surface water that did not interact with wetland sediments. This Cr(VI) would have an isotopic composition similar to that of the cooling tower discharge.

Cr(VI) reduction in the vadose zone is favored by the presence of Fe(II)-bearing minerals (Eary and Rai, 1989, Pettine et al., 1998 and Raddatz et al., 2011). Total iron concentrations (Fe speciation measurements have not been performed) and mineralogy for stratigraphic units present in the vadose zone and the regional aquifer are shown in Supplementary Fig. 2. The Cerros del Rio basalts have the greatest potential to reduce Cr(VI) to Cr(III) because of the abundance of Fe(II)-bearing minerals such as olivine, pyroxene, and magnetite. When Fe(II) is oxidized to Fe(III), Cr(VI) can be simultaneously reduced to Cr(III). Fe(II)-bearing minerals and glass in Cerros del Rio basalts and in dacitic lithologies of the Puye Formation provide significant reducing potential (cf. Raddatz et al., 2011). Evidence for reduction in vadose zone stratigraphic units, particularly in the Cerros del Rio basalts is shown in Supplementary Fig. 3 (See Supplementary information for discussion). Regional aquifer sediments also contain Fe(II)-bearing minerals (mostly pyroxenes) capable of reducing Cr(VI) to Cr(III) (Supplementary Fig. 2), and the possibility of regional aquifer reduction is suggested by the modeling results of Vesselinov et al. (2013).

It is often assumed that reduction occurs at dissolved oxygen levels of less than 6 ppm, although it can also occur in reducing microenvironments within oxidizing settings or through the metabolic activity of aerobic microbes (Desjardin et al., 2002, Horton et al., 2006 and Raddatz et al., 2011). Reduction by Fe(II) can occur in the presence of dissolved oxygen (Eary and Rai, 1989). In the samples analyzed, dissolved oxygen ranged from ~ 2 mg/L to 10 mg/L.

We postulate that Cr isotopes can be used to understand where in the hydrologic system Cr(VI) reduction occurs. We address this question by evaluating the spatial relationships for Cr(VI) data in 3.2, 3.3, 3.4 and 3.5.

3.2. Background intermediate and regional wells

Wells with background levels of Cr(VI) were identified based on their location relative to the main plume, distribution of plume co-contaminants, and flow and transport considerations. Background wells have Cr(VI) concentrations less than 6 μg/L and $\delta^{53}Cr$ values in the range of 1.2‰–1.9‰ (Fig. 2). These values are similar to those detected at background locations associated with basalts at Idaho National Laboratory (Raddatz et al., 2011) and in the recharge areas of flow paths in alluvial aquifers associated with ultramafic rocks in the western Mojave Desert (Izbicki et al., 2008). Cr mobilized by weathering of tonalitic bedrock in Madagascar also has positive $\delta^{53}Cr$ (Berger and Frei, 2014). Natural background Cr(VI) in LANL groundwater has a higher $\delta^{53}Cr$ signature than industrial chromate sources ($\delta^{53}Cr$ industrial approximately equal to 0‰; Ellis et al., 2002 and Schoenberg et al., 2008), probably as the result of fractionation that occurs during oxidation of Cr(III) to Cr(IV) via water–rock interactions. The deep screens at all dual-screened wells, with the exception of well R-45, have Cr(VI) concentrations and $\delta^{53}Cr$ in the background range, indicating contamination is generally restricted to the uppermost part of the regional aquifer.

3.3. Perched-intermediate wells

Intermediate wells SCI-1 and MCOI-4 are completed in groundwater perched in sedimentary deposits of the Puye Formation above the Cerros del Rio basalts (Supplementary Fig. 1). All other perched-intermediate wells are completed within the basalts, and regional wells are completed in the underlying sedimentary units (Puye Formation or Miocene-age pumiceous sediments) (Supplementary Fig. 1). Well SCI-1 is located along the infiltration pathway from the primary Cr(VI) source associated with Sandia Canyon (Fig. 1). Chromium isotope results from this well are key to understanding where in the hydrologic system reduction occurs. Based on contaminant concentrations, groundwater in well SCI-1 is largely post-1990 in age, thus post-dating

the cessation of Cr(VI) discharges (LANL, 2012). Cr(VI) concentrations present at well SCI-1 consist of vadose-zone Cr that probably represents the tail of the plume. Cr/SO_4 ratios along the primary infiltration pathway are consistent with this interpretation (Supplementary Fig. 4; See Supplementary information for discussion).

Well SCI-1 has the lowest $\delta^{53}Cr$ values observed in this study (0.3‰–0.5‰), suggesting little reduction along the flow pathway to this well. As Cr(VI) in this location represents the tail end of the Cr plume, several conclusions can be drawn: 1) $\delta^{53}Cr$ of the potassium dichromate used in the TA-3 cooling tower was likely approximately zero per mil, consistent with measurements of other industrial Cr sources, 2) whereas Cr(VI) reduction and isotopic fractionation no doubt occurred in the TA-3 cooling tower and in the Sandia Canyon wetland, this fractionation did not lead to significant increases in $\delta^{53}Cr$ in residual Cr(VI) for reasons discussed in Sections 3.1, and 3) only minor reduction is likely to have occurred in the overlying Bandelier Tuff. The distribution of total iron, Fe(II)-bearing minerals and the inferred distribution of Cr(III) in the vadose zone are consistent with minor reduction along the flow path above the Cerros del Rio basalts, with most reduction occurring within and possibly below the basalts (See discussion in Supplementary information and Supplementary Fig. 2 and Supplementary Fig. 3).

Perched-intermediate well MCOI-4 is located along the same perching horizon as well SCI-1 but has a different geochemical signature (LANL, 2012). Water from well MCOI-4 has some of the highest $\delta^{53}Cr$ values observed in this study, and Cr(VI) concentrations slightly above background. These concentrations may be the result of lateral transport from Sandia Canyon along a slow pathway that allowed for significant reduction. Alternatively, the Cr(VI) may be partially derived from the unidentified chromium source located in Effluent Canyon with a flow and transport history quite different from the wells associated with the main plume. Regardless of the source, significant reduction of Cr(VI) is suggested by the higher observed $\delta^{53}Cr$.

Perched-intermediate well MCOI-5 is also likely associated, at least in part, with a Mortandad Canyon source of Cr(VI). MCOI-5 has the highest recent $\delta^{53}Cr$ (2.4‰) and lowest Cr(VI) concentration (2.4 μg/L) of the wells included in this study. This well is completed in basalt, which would provide the reduction potential necessary to produce the observed heavy $\delta^{53}Cr$ and low Cr concentration (Raddatz et al., 2011). Wells SCI-2 and MCOI-6 are also completed in basalt but contain a higher proportion of water from Sandia Canyon. Mixing of plumes could confuse interpretation of $\delta^{53}Cr$ signatures by averaging out the degree of reduction that has occurred from different sources and along different flow paths.

The isotopic composition of industrial chromate sources is unlikely to differ between Mortandad Canyon and Sandia Canyon Therefore, the isotopic variation observed in intermediate wells SCI-2, MCOI-6, MCOI-4, and MCOI-5 is likely a function of their position along the overall Cr transport pathway. Well SCI-2 is near the centroid of the Sandia Canyon plume where the velocity of groundwater flow (residence time), the kinetics of reduction, and the reducing capacity of the basalts only favor modest increases in $\delta^{53}Cr$. The other intermediate wells are closer to plume margins where more extensive reduction of Cr(VI), with associated increases in $\delta^{53}Cr$, is likely to occur due to higher availability of Fe(II) reductants (relative to Cr(VI) concentrations) and lengthier transport pathways. Isotopic fractionation caused by sorption may be responsible for small $\delta^{53}Cr$ shifts in some vadose zone samples near the plume boundary. Ellis et al. (2004) found that equilibrium sorption has very little effect on $^{53}Cr/^{52}Cr$ ratios; the effect was not detected at a precision of ± 0.04‰. However, they also reported that small sorption-related $^{53}Cr/^{52}Cr$ shifts could be magnified by up to a factor of ten at the leading edges of advancing Cr(VI) plumes. Accordingly, there is some chance that $\delta^{53}Cr$ values in plume edge vadose zone samples are significantly affected by this phenomenon. However, the actual magnitude and direction of sorption effects are not known, and thus we cannot assess the impact of sorption at present. It should be noted that the chromium plume is very heterogeneous in the vadose zone and it is unknown which wells, if any, are truly at the leading edge of an advancing plume where sorption-related effects may be relevant.

3.4. Regional aquifer wells

Most of the regional aquifer wells showing evidence of Cr(VI) contamination have $\delta^{53}Cr$ values that fall in a narrow range, close to 1‰ (Fig. 2). Fig. 3 shows the processes that can affect Cr(VI) concentration and $\delta^{53}Cr$ values, including reduction, mixing with background waters, and sorption. In the figure, the processes act upon a hypothetical high Cr(VI) concentration end member that has not undergone substantial reduction in the vadose zone or regional aquifer. Reduction and mixing in the vadose zone and regional aquifer can increase the $\delta^{53}Cr$ value while decreasing the Cr(VI) concentration relative to the original end member. Sorption does not change $\delta^{53}Cr$ (except perhaps on the very fringes of a plume; see Section 3.3) but decreases the Cr(VI) concentration. Mixing with background waters and reduction are the likely mechanisms that lead to the observed $\delta^{53}Cr$ values close to unity within the area of highest Cr(VI) contamination.

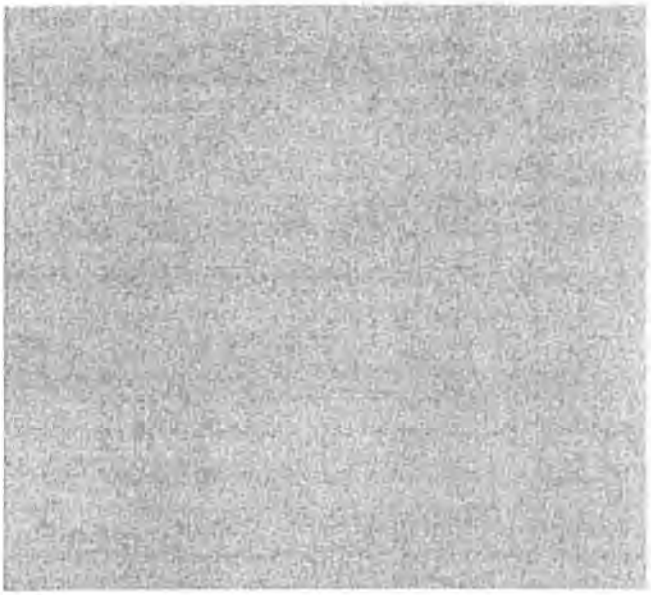

Fig. 3.
$\delta^{53}Cr$ versus Cr(VI) concentration for most recent data from each well. Lower blue curve is a mixing line between a background water and a highly Cr(VI)-contaminated water (open orange box; estimated from the Cr[VI] concentration and $\delta^{53}Cr$ at well R-42; see text for explanation) that has not undergone substantial reduction in the vadose zone or regional aquifer. Upper curve is a mixing line between well R-42 (shows isotopic evidence for Cr(VI) reduction) and background. The isotopic trend associated with reduction for $\varepsilon = 3.4‰$ is shown, along with fraction Cr(VI) remaining as reduction proceeds. The value of 3.4‰ was chosen to be intermediate within the range of experimentally observed fractionation factors. The lack of isotopic fractionation associated with sorption is also shown. Labeled panels with numbers 1, 2, and 3 show expected trends in both $\delta^{53}Cr$ and Cr(VI) concentration for processes of reduction, mixing, and sorption, respectively. These processes likely occur concurrently, at least to some degree. Not all data points are labeled to prevent cluttering of the diagram.

Figure options

A hypothetical high Cr(VI) concentration end member impacting the subsurface was assumed to have an isotopic composition similar to that of well SCI-1 (i.e. $\delta^{53}Cr$ representing an industrial chromate source, possibly with minor isotopic enrichment from reduction in the upgradient cooling tower and wetland). As well R-42 shows the least evidence for reduction in the vadose zone, the isotopic composition and concentration of Cr(VI) in this well were used to estimate the concentration of Cr(VI) entering the perched intermediate aquifer at locations such as well SCI-1. Using δ_0 from well SCI-1 and δ from well R-42, Eq. (1) was used to calculate f, the fraction of Cr(VI) remaining after reduction along the flow path to well R-42. The value of f was then used to estimate the initial concentration of Cr(VI). This calculation ignores the minor effect of mixing with background Cr(VI). While sufficient to illustrate the processes governing observed Cr isotopic variation, the hypothetical end-member, and associated reduction trend, is shown as an example only. Given the spatial and temporal heterogeneity in infiltration and flow pathways and discharge concentrations, the flow path to any individual location

could have experienced lower or higher initial Cr(VI) inputs.

It is clear that reduction occurred somewhere along the individual flow paths in all contaminated wells with the possible exception of well SCI-1 (process 1 in Fig. 3). (It is important to note that Cr isotope measurements do not imply reduction has occurred at the location being sampled but rather somewhere along the flow path to that location.) Except for samples from the deep well screens, the Cr data from all wells in the contaminant plume plot above the mixing line defined by the hypothetical high Cr(VI) source that has not undergone reduction and the regional groundwater background location with the highest $\delta^{53}Cr$. All such waters must have experienced some degree of Cr(VI) reduction as these data cannot be explained by mixing alone (the lower curve in Fig. 3) (cf. Raddatz et al., 2011). It is also clear from comparison of results with the perched-intermediate wells that some of the reduction has occurred in the Cerros del Rio basalts, consistent with the presence of abundant iron(II)-bearing minerals, and potentially in the overlying Puye Formation in the case of well MCOI-4. As Fe(II)-bearing minerals occur in all stratigraphic units, reduction in other units, including the regional aquifer, is also possible. In addition, it is apparent that although background concentrations are low, mixing with background Cr(VI) could explain much of the observed Cr isotope variation. Many of the points fall along the upper mixing line between well R-42 (where evidence for reduction is seen) and the regional groundwater background end-member (process 2 in Fig. 3). Waters at these locations have likely experienced a combination of reduction and mixing with background Cr(VI). Regional aquifer wells near the centroid of mass (e.g., R-28, R-42, and the shallow screen at well R-50) are less affected by mixing with background than wells closer to the periphery of the plume. While an ε value of 3.4‰ is used for illustration purposes in Fig. 3, it should be noted that lower ε effective values may be more representative of field conditions (Berna et al., 2010, Jamieson-Hanes et al., 2012a and Jamieson-Hanes et al., 2012b).

Time series data from the shallow screen at well R-43 are also informative. Increasing Cr(VI) concentration trends with initially decreasing $\delta^{53}Cr$ values are consistent with a recent arrival of the Cr(VI) plume at this location (Fig. 4). As concentrations increase, more contaminant Cr(VI) with a lower $\delta^{53}Cr$ signature relative to background Cr(VI) is present (Fig. 4). Similar trends of decreasing $\delta^{53}Cr$ with increasing Cr(VI) concentration are seen in both screens of well R-45, consistent with plume arrival at this location (Fig. 5). As stated in Section 3.3, the effect of sorption at the plume periphery on observed $\delta^{53}Cr$ is unknown.

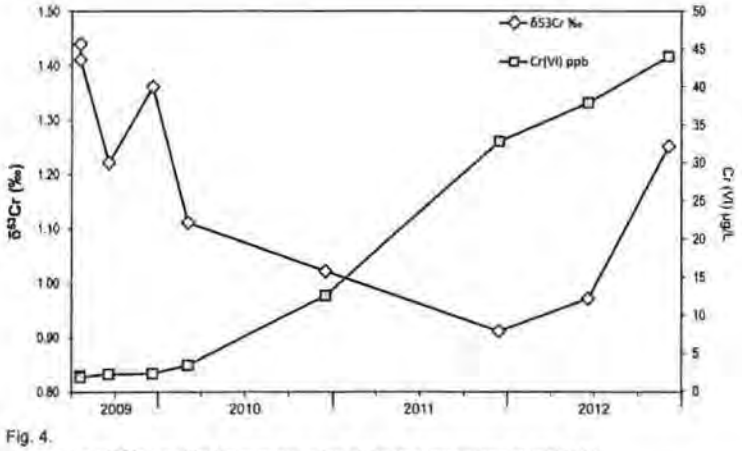

Fig. 4.
Time series of $\delta^{53}Cr$ and Cr(VI) concentration at the shallow screen of well R-43.

Figure options

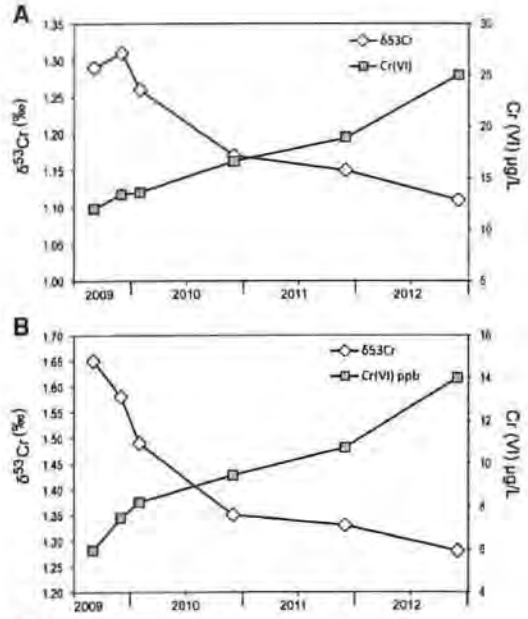

Fig. 5.
Time series of $\delta^{53}Cr$ and Cr(VI) concentration at the shallow screen (A) and deep screen (B) of well R-45.

Figure options

3.5. Location and magnitude of reduction

The isotopic results are consistent with the prevailing conceptual model for this site in which contaminant Cr(VI) undergoes partial reduction in the vadose zone, primarily in the basalts, mixes with background Cr(VI) produced through natural weathering of the rock units, and then percolates into the regional aquifer at multiple arrival points (LANL, 2009 and LANL, 2012). The similarity in $\delta^{53}Cr$ values of contaminated regional aquifer wells could be taken as evidence that little reduction occurs in the regional aquifer. However, the presence of Fe(II)-bearing minerals in regional aquifer sediments makes it likely for some degree of reduction to occur, (Supplementary Fig. 2), unless such reduction capacity has been overwhelmed by ongoing inputs of Cr(VI).

The reduction capacity and kinetics of reduction in the vadose zone and regional aquifer are insufficient to completely attenuate the Cr(VI) plume as demonstrated by high concentrations at wells such as R-42. Using Eq. (1) and assuming δ_0 of 0‰ and $\varepsilon = 3.4$‰, it can be estimated that about 25% reduction of initial Cr(VI) has occurred along the entire flow path (cooling tower to regional aquifer) to R-42. If a lower value of $\varepsilon = 2$‰ is used instead, the degree of reduction increases to approximately 40%. Note that the degree of reduction for well R-42 shown on the reduction vector in Fig. 3 is for reduction in the vadose zone and regional aquifer only. The data presented herein represent a recent snapshot in time. It is unknown if the reduction capacity of the system has become less reactive over time due, for example, to armoring with Cr hydroxides or if the kinetics of reduction in the system have always been relatively slow.

It is possible that the preceding calculations underestimate the true degree of reduction that has occurred. For example, if the actual ε value prevalent in LANL groundwater is significantly less than 3.4‰, the magnitude of reduction would be underestimated. A recent quantitative reactive transport modeling study has demonstrated that low effective epsilon values are associated with higher reduction rates and/or transport limitations (Wanner and Sonnenthal, 2013). In addition, Rayleigh models may underestimate reduction by several percent because of the assumption of closed system behavior (Abe and Hunkeler, 2006). The apparent lack of isotopic enrichment in the regional aquifer associated with the similarity in regional aquifer $\delta^{53}Cr$ measurements could reflect, in part, constant Cr(VI) inputs via multiple breakthrough points from the vadose zone to the regional aquifer over a wide area (Vesselinov et al., 2013). Similarly, the effective, field-relevant value of ε may be a factor of two or more less than that derived from laboratory

batch experiments because of reservoir effects associated with possible diffusion of Cr(VI) into reducing microenvironments, thus causing significant underestimation of reduction (Clark and Johnson, 2008 and Berna et al., 2010).

4. Conclusions

Chromium isotopic measurements of LANL groundwaters provide strong evidence for reduction of Cr(VI) in vadose zone basalts, and possibly in other stratigraphic units containing Fe(II)-bearing minerals. Reduction and mixing with background Cr(VI) are important processes leading to observed Cr isotopic variation. Though the reducing capacity of the various volcanic and sedimentary units is significant, it is insufficient for complete natural attenuation of the Cr(VI) plume. The kinetics of reduction may be relatively slow or the reduction capacity may have been overwhelmed by the large mass and potentially higher historic concentrations of Cr(VI) that passed through the system. Alternatively, isolation of reduction capacity from groundwater (e.g., by armoring with precipitated Cr hydroxides or preferential flow bypassing reduction sites) may have occurred. Precise double-spiked Cr isotope analyses of Cr(VI) are a powerful tool to identify where in a hydrologic system Cr(VI) reduction is occurring. A fuller understanding of site-specific isotopic enrichment factors and fractionation models will improve the potential for quantitative estimates of Cr(VI) reduction.

Given the small number of previous publications on the usage of Cr isotopes to detect Cr(VI) reduction, this study provides insight into the effective use of this new approach and the potential for Cr(VI) reduction in certain systems. Our data interpretation is somewhat complex, making use of a detailed understanding of groundwater flow paths and the potential for multiple Cr(VI) sources. We suggest this level of complexity may be common in future applications of Cr isotope measurements in complex groundwater flow regimes. However, we emphasize that in complex flow regimes, constraining Cr(VI) reduction via Cr(VI) concentration data alone is even more difficult than in simple systems, making the isotopic approach all the more valuable. Finally, the use of multiple chemical data (e.g., Cr(VI)/sulfate ratios) can provide additional constraints to improve the interpretation of Cr isotope data.

The following are the supplementary data related to this article.

Supplementary information

Help with DOCX files — Options

Supplementary Fig. 1.

Geologic cross-section along the primary Cr(VI) flow pathway with contaminant pathways shown. SCC-2 is a corehole that is approximately colocated with well SCI-2.

Help with ZIP files — Options

Supplementary Fig. 2.

Elemental Capture Spectroscopy (ECS) log of iron from well R-28. XRF data from wells R-15 and R-12 have been extrapolated onto this log for comparison. Fe(II)-bearing minerals present in each unit are shown along with most recent $\delta^{53}Cr$ values from wells SCI-1, SCI-2, R-42, and R-28 (extrapolated based on their relative positions in the stratigraphic column). Note that SCI-1 is actually completed in a perched aquifer located at the top of the Cerros del Rio basalts in Puye sediments.

Help with ZIP files — Options

Supplementary Fig. 3.

Stratigraphy at SCC-2/SCI-2, moisture profile, and total Cr profiles for DI water leach and EPA Method 3050 digestion from core at this locality. DI and 3050 leach values for Cerros del Rio basalts from uncontaminated areas are shown.

Help with ZIP files Options

Supplementary Fig. 4.

Cr/SO4 for surface waters (locations SCS-2 and SCS-3) and alluvial water (SCA-2) and for wells along the primary flow path of the Cr plume.

Help with PDF files Options

Acknowledgments

This work was funded as part of the U.S. Department of Energy's investigation of legacy contamination at Los Alamos National Laboratory. This manuscript benefited significantly from the input of two anonymous reviewers.

References

Abe and Hunkeler, 2006 Y. Abe, D. Hunkeler
Does the Rayleigh equation apply to evaluate field isotope data in contaminant hydrogeology?
Environ. Sci. Technol., 40 (2006), pp. 1588–1596

View Record in Scopus | Full Text via CrossRef | Citing articles (65)

Basu and Johnson, 2012 A. Basu, T.M. Johnson
Determination of hexavalent chromium reduction using Cr stable isotopes: Isotopic fractionation factors for permeable reactive barrier materials
Environ. Sci. Technol., 46 (10) (2012), pp. 5353–5360

View Record in Scopus | Citing articles (21)

Berger and Frei, 2014 A. Berger, R. Frei
The fate of chromium during tropical weathering: a laterite profile from Central Madagascar
Geoderma, 213 (2014), pp. 521–532

Article | PDF (1771 K) | View Record in Scopus | Citing articles (11)

Berna et al., 2010 E.C. Berna, T.M. Johnson, R.S. Makdisi, A. Basu
Cr stable isotopes as indicators of Cr(VI) reduction in groundwater: a detailed time-series study of a point-source plume
Environ. Sci. Technol., 44 (3) (2010), pp. 1043–1048

View Record in Scopus | Full Text via CrossRef | Citing articles (32)

Birdsell et al., 2005 K.H. Birdsell, B.D. Newman, D.E. Broxton, B.A. Robinson
Conceptual models of vadose zone flow and transport beneath the Pajarito Plateau, Los Alamos, New Mexico
Vadose Zone J., 4 (3) (2005), pp. 620–636

View Record in Scopus | Full Text via CrossRef | Citing articles (19)

Blowes, 2002 D. Blowes
Environmental chemistry — tracking hexavalent Cr in groundwater
Science, 295 (5562) (2002), pp. 2024–2025

View Record in Scopus | Full Text via CrossRef | Citing articles (76)

Broxton and Vaniman, 2005 D.E. Broxton, D.T. Vaniman
Geologic framework of a groundwater system on the margin of a rift basin, Pajarito Plateau, north-central New Mexico
Vadose Zone J., 4 (3) (2005), pp. 522–550

View Record in Scopus | Full Text via CrossRef | Citing articles (29)

Clark and Johnson, 2008 S.K. Clark, T.M. Johnson
Effective isotopic fractionation factors for solute removal by reactive sediments: a laboratory microcosm and slurry study

Environ. Sci. Technol., 42 (21) (2008), pp. 7850–7855

View Record in Scopus | Full Text via CrossRef | Citing articles (29)

Dale et al., 2013 M. Dale, P. Longmire, K. Granzow, S. Yanicak, R. Mayer
Statistical Analysis of Regional Aquifer Background, Pajarito Plateau, New Mexico
2013 GSA Annual Meeting, Denver, CO (2013)

Davis and Olsen, 1995 A. Davis, R.L. Olsen
The geochemistry of chromium migration and remediation in the subsurface
Ground Water, 33 (5) (1995), pp. 759–768

View Record in Scopus | Full Text via CrossRef | Citing articles (44)

Desjardin et al., 2002 V. Desjardin, R. Bayard, N. Huck, A. Manceau, R. Gourdon
Effect of microbial activity on the mobility of chromium in soils
Waste Manag., 22 (2) (2002), pp. 195–200

Article | PDF (159 K) | View Record in Scopus | Citing articles (34)

Dossing et al., 2011 L.N. Dossing, K. Dideriksen, S.L.S. Stipp, R. Frei
Reduction of hexavalent chromium by ferrous iron: a process of chromium isotope fractionation and its relevance to natural environments
Chem. Geol., 285 (1–4) (2011), pp. 157–166

Article | PDF (907 K) | View Record in Scopus | Citing articles (32)

Eary and Rai, 1989 L.E. Eary, D. Rai
Kinetics of chromate reduction by ferrous ions derived from hematite and biotite at 25 °C
Am. J. Sci., 289 (2) (1989), pp. 180–213

Full Text via CrossRef

Ellis et al., 2002 A.S. Ellis, T.M. Johnson, T.D. Bullen
Chromium isotopes and the fate of hexavalent chromium in the environment
Science, 295 (5562) (2002), pp. 2060–2062

View Record in Scopus | Full Text via CrossRef | Citing articles (157)

Ellis et al., 2004 A.S. Ellis, T.M. Johnson, T.D. Bullen
Using chromium stable isotope ratios to quantify Cr(VI) reduction: lack of sorption effects
Environ. Sci. Technol., 38 (13) (2004), pp. 3604–3607

View Record in Scopus | Full Text via CrossRef | Citing articles (59)

Gao et al., 2010 Y. Gao, T. Ma, W. Ling, C. Liu, L. Li
Analytical method of Cr stable isotope and its application to water pollution survey
Chin. Sci. Bull., 55 (7) (2010), pp. 664–669

View Record in Scopus | Full Text via CrossRef | Citing articles (4)

Han et al., 2012 R. Han, L. Qin, S.T. Brown, J.N. Christensen, H.R. Beller
Differential isotopic fractionation during Cr (VI) reduction by an aquifer-derived bacterium under aerobic versus denitrifying conditions
Appl. Environ. Microbiol., 78 (2012), pp. 2462–2464

View Record in Scopus | Full Text via CrossRef | Citing articles (10)

Horton et al., 2006 R.N. Horton, W.A. Apel, V.S. Thompson, P.P. Sheridan
Low temperature reduction of hexavalent chromium by a microbial enrichment consortium and a novel strain of *Arthrobacter aurescens*
BMC Microbiol., 6 (2006), p. 5

View Record in Scopus | Full Text via CrossRef | Citing articles (8)

Izbicki et al., 2008 J.A. Izbicki, J.W. Ball, T.D. Bullen, S.J. Sutley
Chromium, chromium isotopes and selected trace elements, western Mojave Desert, USA
Appl. Geochem., 23 (5) (2008), pp. 1325–1352

Article | PDF (1576 K) | View Record in Scopus | Citing articles (66)

Izbicki et al., 2012 J.A. Izbicki, T.D. Bullen, P. Martin, B. Schroth
Delta Chromium-53/52 isotopic composition of native and contaminated groundwater, Mojave Desert, USA
Appl. Geochem., 27 (4) (2012), pp. 841–853

Article | PDF (1939 K) | View Record in Scopus | Citing articles (16)

Jamieson-Hanes et al., 2012a J.H. Jamieson-Hanes, R.T. Amos, D.W. Blowes
Reactive transport modeling of chromium isotope fractionation during Cr(VI) reduction
Environ. Sci. Technol., 46 (24) (2012), pp. 13311–13316

View Record in Scopus | Full Text via CrossRef | Citing articles (8)

Jamieson-Hanes et al., 2012b J.H. Jamieson-Hanes, B.D. Gibson, M.B.J. Lindsay, Y. Kim, C.J. Ptacek, D.W. Blowes
Chromium isotope fractionation during reduction of Cr(VI) under saturated flow conditions
Environ. Sci. Technol., 46 (12) (2012), pp. 6783–6789

View Record in Scopus | Full Text via CrossRef | Citing articles (8)

Johnson and Bullen, 2004 T.M. Johnson, T.D. Bullen
Mass-dependent fractionation of selenium and chromium isotopes in low-temperature environments
C.M. Johnson, B.L. Beard, F. Albarede (Eds.), Rev. Mineral. Geochem., 55 (1) (2004), pp. 289–317

View Record in Scopus | Full Text via CrossRef | Citing articles (5)

Kitchen et al., 2012 J.W. Kitchen, T.M. Johnson, T.D. Bullen, J.M. Zhu, A. Raddatz
Chromium isotope fractionation factors for reduction of Cr(VI) by aqueous Fe(II) and organic molecules
Geochim. Cosmochim. Acta, 89 (2012), pp. 190–201

Article | PDF (531 K) | View Record in Scopus | Citing articles (22)

LANL, 2007 LANL
Summary of Sandia Canyon Phase I Sediment Investigations, LA-UR-07-6019
Los Alamos, New Mexico (2007)

LANL, 2009 LANL
Investigation Report for Sandia Canyon, LA-UR-09-6450
Los Alamos, New Mexico (2009)

LANL, 2012 LANL
Phase II Investigation Report for Sandia Canyon, LA-UR-12-24593
Los Alamos, New Mexico (2012)

Palmer and Puls, 1994 C.D. Palmer, R.W. Puls
Natural attenuation of hexavalent chromium in groundwater and soils
EPA Groundwater Issue Paper, US Environmental Protection Agency, Washington, D.C., USA (1994)

Palmer and Wittbrodt, 1991 C.D. Palmer, P.R. Wittbrodt
Processes affecting the remediation of chromium-contaminated sites
Environ. Health Perspect., 92 (1991), pp. 25–40

View Record in Scopus | Full Text via CrossRef | Citing articles (262)

Pettine et al., 1998 M. Pettine, L. D'Ottone, L. Campanella, F.J. Millero, R. Passino
The reduction of chromium (VI) by iron (II) in aqueous solutions
Geochim. Cosmochim. Acta, 62 (9) (1998), pp. 1509–1519

Article | PDF (267 K) | View Record in Scopus | Citing articles (110)

Raddatz et al., 2011 A.L. Raddatz, T.M. Johnson, T.L. McLing
Cr stable isotopes in Snake River Plain aquifer groundwater: evidence for natural reduction of dissolved Cr(VI)
Environ. Sci. Technol., 45 (2) (2011), pp. 502–507

View Record in Scopus | Full Text via CrossRef | Citing articles (19)

Schoenberg et al., 2008 R. Schoenberg, S. Zink, M. Staubwasser, F. von Blanckenburg
The stable Cr isotope inventory of solid Earth reservoirs determined by double spike MC-ICP-MS
Chem. Geol., 249 (3–4) (2008), pp. 294–306

Article | PDF (732 K) | View Record in Scopus | Citing articles (72)

Sikora et al., 2008 E.R. Sikora, T.M. Johnson, T.D. Bullen
Microbial mass-dependent fractionation of chromium isotopes
Geochim. Cosmochim. Acta, 72 (15) (2008), pp. 3631–3641

Article | PDF (215 K) | View Record in Scopus | Citing articles (47)

Vesselinov et al., 2013 V.V. Vesselinov, D. Katzman, D. Broxton, K. Birdsell, S. Reneau, D. Vaniman, P. Longmire, J. Fabryka-Martin, J. Heikoop, M. Ding, D. Hickmott, E. Jacobs, T. Goering, D. Harp, P. Mishra
Data and Model-driven Decision Support for Environmental Management of a Chromium Plume at Los Alamos National Laboratory Waste Management Symposium 2013, Session 109, February 24–28, 2013, Phoenix, AZ, USA (2013)

Wanner et al., 2012a C. Wanner, U. Eggenberger, D. Kurz, S. Zink, U. Mäder
A chromate-contaminated site in southern Switzerland — part 1: site characterization and the use of Cr isotopes to delineate fate and transport
Appl. Geochem., 27 (3) (2012), pp. 644–654

Article | PDF (809 K) | View Record in Scopus | Citing articles (17)

Wanner et al., 2012b C. Wanner, S. Zink, U. Eggenberger, U. Mäder
Assessing the Cr(VI) reduction efficiency of a permeable reactive barrier using Cr isotope measurements and 2D reactive transport modeling
J. Contam. Hydrol., 131 (1–4) (2012), pp. 54–63

Article | PDF (1073 K) | View Record in Scopus | Citing articles (12)

Wanner and Sonnenthal, 2013 C. Wanner, E.L. Sonnenthal
Assessing the control on the effective kinetic Cr isotope fractionation factor: a reactive transport modeling approach
Chem. Geol., 337–338 (2013), pp. 88–98

Article | PDF (1233 K) | View Record in Scopus | Citing articles (12)

Zink et al., 2010 S. Zink, R. Schoenberg, M. Staubwasser
Isotopic fractionation and reaction kinetics between Cr(III) and Cr(VI) in aqueous media
Geochim. Cosmochim. Acta, 74 (20) (2010), pp. 5729–5745

Article | PDF (835 K) | View Record in Scopus | Citing articles (44)

Corresponding author. Tel.: + 1 505 667 8128.

1 Present address: DOE Oversight Bureau-New Mexico Environment Department, 1183 Diamond Drive, Suite B, Los Alamos, NM 87544, USA.

2 Present address: Center for Plasma Mass Spectrometry, University of California Davis, Department of Geology, One Shields Avenue, Davis, CA 95616, USA.

3 Present address: Center for Isotope Geochemistry, University of California, Berkeley and Lawrence Berkeley National Lab, 485 McCone Hall, Berkeley, CA 94720, USA.